

UCSF

UC San Francisco Previously Published Works

Title

Awake replay of remote experiences in the hippocampus.

Permalink

<https://escholarship.org/uc/item/88q0v5dq>

Journal

Nature neuroscience, 12(7)

ISSN

1097-6256

Authors

Karlsson, Mattias P
Frank, Loren M

Publication Date

2009-07-01

DOI

10.1038/nn.2344

Peer reviewed



HHS Public Access

Author manuscript

Nat Neurosci. Author manuscript; available in PMC 2010 January 01.

Published in final edited form as:

Nat Neurosci. 2009 July ; 12(7): 913–918. doi:10.1038/nn.2344.

Awake replay of remote experiences in the hippocampus

Mattias P. Karlsson and Loren M. Frank

W.M. Keck Center for Integrative Neuroscience and Department of Physiology, University of California, San Francisco, CA 94143-0444

Abstract

Hippocampal replay is thought to be essential for the consolidation of event memories in hippocampal–neocortical networks. Replay is present during both sleep and waking behavior, but while sleep replay involves the reactivation of stored representations in the absence of specific sensory inputs, awake replay is thought to depend on sensory input from the current environment. Here we show that stored representations are reactivated during both waking and sleep replay. We found frequent awake replay of sequences of rat hippocampal place cells from a previous experience. This spatially remote replay was as common as local replay of the current environment and was most robust when the animal had recently been in motion as compared to during extended periods of quiescence. These results indicate that the hippocampus consistently replays past experiences during brief pauses in waking behavior, suggesting a role for waking replay in memory consolidation and retrieval.

Introduction

The hippocampus is essential for the formation of long term memories for events^{1, 2}. This process is thought to involve rapid encoding in highly plastic hippocampal circuits followed by a consolidation process where hippocampal representations are “reactivated”, allowing these patterns to be engrained in less plastic hippocampal – neocortical circuits^{3, 4}. Reactivation is hypothesized to depend on hippocampal sharp wave – ripple (SWR) events^{5–8} because SWRs propagate from the hippocampus to adjacent cortical regions^{9, 10} and include firing patterns associated with previous^{6, 11–16} as well as current experiences^{17–19}.

Reactivation has been observed in ensembles of simultaneously recorded hippocampal place cells. These spatial reactivation events have been separated into two categories: events that occur outside of an environment (following the experience) and events that occur within the environment (during the experience). Studies of reactivation outside the reactivated environment have focused largely on sleep and extended periods of awake immobility where reactivation can occur in the absence of the original sensory inputs. During these periods hippocampal place cells that fire together during exploration tend to fire together afterwards

Users may view, print, copy, and download text and data-mine the content in such documents, for the purposes of academic research, subject always to the full Conditions of use:http://www.nature.com/authors/editorial_policies/license.html#terms

Author Contributions

M.K and L.F. designed the experimental paradigm; M.K. carried out all of the data collection and the majority of the analyses; L.F. carried out the remaining analyses; M.K. and L.F. wrote the manuscript.

during SWRs⁶, 11–13. Complementary studies have shown that entire sequences can be replayed at high speeds^{14–16}, 19.

Reactivation within an environment, in contrast, has been associated with current sensory inputs^{17–19}. Recent studies observed awake replay events beginning with activation of cells whose place fields were close to the animal and progressing to cells with place fields farther away. These observations led to the hypothesis that awake replay, unlike replay in sleep or sleep-like states, is a result of sequential activation of sensory driven place fields. One model suggests that the progressive increase in hippocampal depolarization during a SWR^{9, 10} causes cells with place fields close to the animal (and thus with membrane potentials close to threshold) to fire first. Cells with place fields farther away start from a less depolarized potential and would therefore require more input and a longer time to become active^{17–19}.

But is awake replay always dependent on sensory inputs? If instead awake and sleep replay both activate stored representations of past experiences, we would expect that animals could replay experiences of one place while awake in a different place. We therefore examined replay of hippocampal place cell sequences from the CA3 and CA1 regions of the hippocampus during waking experience across multiple environments. We found robust remote replay of past experiences during waking behavior consistent with a role for awake replay in memory retrieval and consolidation.

Results

We recorded ensembles of principle neurons from hippocampal areas CA3 and CA1 while animals were sequentially exposed to two physically different W-shaped environments (“run sessions” in E1 and E2) and during intervening sessions in a high walled rest box (Fig. 1)²⁰. Each animal was exposed to E2 for two run sessions a day across either three (animal 1) or six (animals 2 & 3) consecutive days before the first exposure to E1, so E1 was always more novel than E2. The environments were oriented at 90 degrees with respect to one another and were separated by a high barrier so the animal had access to largely distinct sets of visual cues from each environment (Supplementary Fig. 1). This layout helped ensure that the two environments were associated with distinct hippocampal representations (see below). Each environment had one reward site at the endpoint of each arm and animals were rewarded for performing a continuous alternation task^{20–22}. Data presented here were recorded on the day of the first exposure to E1 and the days thereafter (Supplementary Fig. 2).

We restricted our analyses to putative excitatory neurons with clear place specific firing and stable clusters. To avoid confusing replay events and sequential firing during movement-related phase precession²³, we examined SWRs that occurred when animals were moving less than 2 cm/sec. Individual cells had very similar patterns of spatial activity across the two exposures to E1 but generally very different patterns in E1 and E2 (Fig. 1b and Supplementary Fig. 3). We initially combined CA3 and CA1 cells into a single population to maximize the number of neurons active during each SWR.

Awake replay in E1

Place specificity led to sequences of neural activity as the animal moves through the environment (Fig. 2a,b). Replay of these sequences can only be detected if a sufficient number of cells with place fields are activated, so we defined candidate replay events as SWRs activating 5 or more cells with place fields in E1. We divided candidate events into 15 ms bins and used a simple Bayesian decoder^{24, 25} with a uniform prior to translate the ensemble spiking into probability distributions over positions in E1. We then determined the likelihood that the ordered firing seen during a candidate event corresponded to a coherent spatial sequence. Sequences of ordered positions that were unlikely to occur by chance ($p < 0.05$) were considered to represent replay (see Methods).

We found robust and frequent awake replay of E1 during both the first (Fig. 2c–f) and second (Supplementary Table 1) exposure on each day. We ordered place cells by the distance of each cell's place field peak from the endpoint of the center arm of E117–19 (Fig. 2d). Thus, individual replay events are visible as diagonal sweeps of spike trains. In rare occasions the trajectory corresponding to a sweep went from one outer arm to the other, in which case the cells were ordered as a function of the distance from the end of an outer arm. Overlapping SWRs were combined across tetrodes, so many events extended beyond the SWR seen on a single tetrode.

In total, 288 (47%) of 612 candidate events during the first exposure to E1 involved significant replay of E1. We refer to these events as “local replay” to distinguish them from “remote replay” where sequences from E1 were replayed while the animal was in a different environment (see below). The proportion of significant events is much greater than the 5% expected by chance ($Z = 20.85$, $p < 10^{-10}$) and similar to that seen in previous studies^{17, 18}. These events occurred throughout the track and were prevalent at the “choice point” where animals coming from the food well on the center arm of the maze had to choose an outside arm to visit (Supplementary Fig. 4). Thus, these events may be similar to the vicarious trial and error activity reported previously²⁶ (see Supplemental Results). As in previous studies of novel environments²⁷ and awake replay¹⁷, the majority of the place cells recorded were active in both directions of motion (e.g. Fig. 2a). We chose not to apply a specific criterion to separate unidirectional and bidirectional cells and thus we did not classify events as either forward or reverse replay^{17, 18}.

Awake and quiescent replay of E1 in the rest box

We found robust and frequent replay of E1 in SWRs occurring during awake periods in the rest box. We first combined data from Rest 2 and Rest 3. To be conservative, awake periods were defined as times when animals had been immobile no more than five seconds. In SWRs occurring during these periods we observed clear sequential replay of E1 place fields (Fig. 2g–n). Two hundred fifty six (44.1%) of 580 candidate events showed significant replay of E1 during awake periods in the rest box, significantly more than chance ($Z = 15.48$, $p < 10^{-10}$). These awake replay events occurred consistently across all three animals (animal 1, 5/22 events; animal 2, 149/346 events; animal 3, 102/212 events; all $> 5\%$, p 's $< .05$). The proportion of significant events was not different than the 47% for run sessions in

E1 (rest vs. E1: $Z = 1.01$, N.S.) and these events represented physically possible trajectories on the track (see Supplemental Results).

We then compared the prevalence of replay during these awake episodes with replay during more extended periods of immobility in the rest box. In the absence of EMG data, we chose to be conservative and labeled these periods as “quiescent”. We first defined periods of quiescence as times when animals had been immobile for five seconds or longer. This threshold was chosen to capture short periods of sleep (Supplementary Fig. 5a–d), but also likely included a number of awake periods.

The commonly accepted idea that memory reactivation occurs primarily during sleep-like states led us to expect that replay activity would be most robust during quiescence. In actuality, replay of E1 during quiescent SWRs was less likely to occur: 373 of 1046 (35.7%) candidate events showed significant replay (Fig. 3a; awake (44.1%) > quiescence, $Z = 3.36$, $p < 0.001$). We also used a more stringent criterion for quiescence (immobility for more than 60 seconds) with the same results (106 of 310 events, 34.2%, awake > quiescence, $Z = 2.88$, $p < 0.005$).

The observed difference was not due to a lack of activity from E1 place cells during quiescence, as for 217 of 244 cells, rates were higher during quiescent as compared to awake SWRs (Fig. 3b; $Z = 9.34$, $p < 10^{-10}$). Given the occurrence of a candidate event, however, fewer place cells were active in individual quiescent events than in individual awake events (Fig. 3c; Rank-sum, $Z = 6.65$, $p < 10^{-10}$). Thus, while the overall rate of spiking during SWRs is lower in the awake state, neuronal activation tends to be more concentrated in select SWRs.

While the comparison of the number of replay events for the same population of place cells is meaningful, the absolute number of replay events detected on a day will depend on the total number of neurons with place fields recorded. We therefore developed a complementary pair-wise analysis approach that is much less sensitive to these sampling issues. We calculated an R^2 value which describes the extent to which the distance between the peaks of two neurons' place fields predicts the timing of their SWR spikes (see Methods). We also used a modified version of that analysis to visualize pairwise activity. We computed cross-correlation histograms of spike trains from all pairwise combinations of simultaneously recorded place cells and plotted the normalized histograms as a function of the linear distance between the place field peaks²⁸ (see Methods). The pair-wise signature of replay is an expanding ‘V’ centered at 0 ms latency. The resulting plots for awake and quiescent SWRs suggested that awake SWRs were more structured (Fig. 3d).

We quantified that impression and found that E1 place field distances were more strongly predictive of the time between SWR spikes during wakefulness than quiescence at both the 5 and 60 second immobility thresholds (awake $R^2 = 0.1164$, 70803 spike pairs, 5442 SWRs; quiescent 5 second threshold $R^2 = 0.0693$, 99598 spike pairs, 28003 SWRs; quiescent 60 second threshold $R^2 = 0.0875$, 23908 spike pairs, 15074 SWRs, awake > quiescent p 's < 10^{-10}). The two quiescent R^2 values were also significantly different ($Z = 4.90$, $p < 10^{-7}$), suggesting that at a pair-wise level the strength of replay varies as a function of the length of

immobility. The difference in awake and quiescent replay could not be explained by clustering errors, cluster instability or decay in replay strength as a function of the time since the E1 experience (see Supplementary Results and Supplementary Clusters).

Awake replay of E1 in E2

We then asked whether E1 replay could continue during performance of the alternation task in E2. Despite the distinct representations of E1 and E2, when animals were located in E2 182 (41.2%) of 442 candidate replay events showed significant replay of E1 ($Z = 12.67$, $p < 10^{-10}$ compared to chance; Fig. 4a–l, Supplementary Fig. 6 and Supplementary Fig. 7). As expected, there were also many replays of E2: 147 (44.6%) of 330 candidate events were significant ($Z = 14.45$, $p < 10^{-10}$). Replay in E2 was not affected by immobility time (see Supplementary Results and Supplementary Figure 5b), suggesting any brief periods of quiescence in E2 had little effect on the overall proportion of replay events of either E1 or E2.

We confirmed these results using the pair-wise analysis which showed a clear relationship between E1 place field distance and pair-wise spike timing of E1 place cells during SWRs in E2 (Fig. 4m). Here, we focused on E1 place cells that did not have place fields in E2, so these cells were active primarily during SWRs. The pair-wise regression analysis for E1 cells yielded a higher R^2 value in E2 than for awake periods in the rest box (regression $R^2 = 0.1736$, 19850 spike pairs, 18512 SWRs, compared to rest, $Z = 8.57$, $p < 10^{-10}$). Finally, we also applied the pair-wise measure to CA3 and CA1 neurons separately and found clear evidence for sequential activity in both regions as well as stronger pair-wise correlations in CA3 than in CA1 (See Supplementary Results and Supplementary Fig. 8).

The prevalence of E1 replay events in E2 led us to ask whether E1 replay was related to replay of E2. While most significant replay events replayed only one track (Fig. 4e,f,k,l), 24 replayed both tracks simultaneously (24 / 182 replay events for E1 (13.2%) and 24 / 147 events for E2 (16.3%)). To determine whether E1 and E2 replay occurred together more often than expected by chance we examined all events that were candidates for both E1 and E2 replay. We found that the p-values for E1 and E2 decoding regressions were not correlated ($R = 0.07$, N.S.; see Methods). We also asked, for each event that was a candidate for both E1 and E2, whether the p-value for the E1 replay was related to the number of E2 cells active, as might be expected if coherent E1 replay suppressed E2 activity. The correlation was not significantly different than 0 ($R = 0.05$, N.S.). Thus, joint replay appears to result from independent replay of E1 and E2.

We then asked whether the direction of replay in E1 was related to the animal's location in E2. We reasoned that at times when an animal was located at one of the three endpoints of the W-track, replay initiated at the animal's location must represent travel in the direction extending away from that endpoint. Thus, we used the direction of the decoded replay (toward or away from the center arm food well) to determine whether replay of E1 could have initiated at a corresponding location in E2.

While most E1 replay events occurring while the animal was in E1 moved away from the animal's position 17–19 (151 of 190 events, 79.5%; more than half: $Z = 6.01$, $p < 10^{-8}$),

20.5% did not (Supplementary Fig. 9). Further, E1 replay events in E2 moved away from the animal's corresponding location in E1 only about half the time (85 of 158 events, 53.8%, not greater than 50%, $Z = 0.68$, N.S.). Thus, nearly half of the E1 events in E2 were decoded as moving towards the corresponding position of the animal in E1. Similarly, for the 24 events where both tracks were replayed simultaneously, the direction of the pairs of E1/E2 replay events was not significantly correlated ($R = 0.34$; N.S.). None of these effects could be attributed to clustering errors or cluster instability (see Supplementary Results and Supplementary Clusters).

Replay in the final and initial rest sessions

Following exposure to E2, animals were placed in the rest box one last time. Here, we observed significant awake replay of both environments, with 51 / 147 (34.7%) significant candidate E1 events and 58 / 128 (45.3%) significant candidate E2 events. Once again, E1 and E2 appeared to be replayed independently (see Supplementary Results). The decline in the proportion of E1 replay events as compared to the previous rest was significant ($Z = 2.07$, $p < 0.04$). There was, however, no corresponding decline in the pair-wise awake correlation measure applied to cells with E1 but not E2 place fields (Rest 4 $R^2 = 0.1129$, 14631 spike pairs, Rest 2 & 3 $R^2 = 0.1164$, 70803 spike pairs; $Z = 0.50$, N.S.). As in the previous rests, the probability of replay and the quality of the pair-wise sequential activity was significantly lower during quiescence (5 second immobility criterion; E1 replay: 87/389 (22.4%) < 34.7% awake, $Z = 2.91$, $p < 0.01$, quiescent $R^2 = 0.0604$, $p < 10^{-10}$ compared to awake; E2 replay: 105/303 (34.7%) < 45.3% awake, $Z = 2.09$, $p < 0.05$).

While replay continued into the final rest, we observed minimal replay activity for either environment during the first rest session of the day. The pair-wise regression yielded a significantly lower R^2 value than for all subsequent behavioral sessions (regression $R^2 = 0.025$; compared to quiescence in rest box, $Z = 8.30$; to awake periods in rest box, $Z = 15.25$; to runs in E2, $Z = 19.13$; all p 's $> 10^{-10}$; Supplementary Fig. 10, Supplemental Table 1). Thus, the strength of replay appeared to decay from the end of one day to the next.

Interaction between local spatial input and remote replay

Our analysis to this point indicated that E1 and E2 replay were independent. But could spatial information from the local environment contribute to the initiation of remote replay as it does for local replay? If so, cells that receive stronger spatial inputs at a location might be more depolarized and thus more likely to initiate a replay event. To examine this possibility we took each significant E1 replay event seen in E2 and identified the cells that fired the first and the last spike of the event. We calculated the local spatial firing rate in E2 for both cells, excluding activity in SWRs (see Methods).

We found that, on average, the first cell had a higher local firing rate than the last cell (Rank-sum, $p < 0.002$). We repeated this analysis for the final rest session and found that local rates were higher for the first cell of awake ($p < 0.05$) but not quiescent E1 replay events (Fig. 5). A similar trend was present for both Rest 2 and Rest 3 (Supplementary Figure 11), and local rates were also higher for the first cell of awake but not quiescent

replays of E2 in the rest box (Supplementary Figure 12). This effect did not result from outlier spikes or other potential confounds (See Supplementary Results).

Discussion

We observed coherent spatial replay during SWRs in three different conditions: 1) awake replay of the currently experienced environment, 2) awake replay of a remote environment and 3) quiescent replay of a remote environment. Awake, remote replay continued long after the initial experience and represented a more precise recapitulation of past sequences than replay seen during quiescence. Further, awake, remote replay was very prevalent and the structure of the remote place fields could explain as much as 17% of the variance of SWR spike timing, indicating that activity consistent with replay is present in a substantial fraction of SWRs. These results pose difficulties for models positing that the ordering of spikes within an awake SWR event stems from ordered activation of sensory driven, subthreshold place fields^{17–19}. Our data are instead consistent with a model where replay activates representations of previous experiences during both waking and sleep²⁹.

We found that the initiation of an awake replay sequence is often related to local spatial input at the animal's location, but that the mnemonic content of awake replay can be effectively independent of location. Thus, local inputs could lead to the activation of a set of neurons which then activate other associated neurons that are part of a previously stored memory. We also saw stronger sequential reactivation in CA3 than CA1, and as SWRs generally originate in CA3¹⁰, replay may involve activation of a sequence stored in CA3 associative connections.

What might lead to remote rather than local replay? We and others have found that novel experiences generate a long lasting increase in neuronal excitability and neuronal coordination for the cells active during those experiences^{13, 17, 20, 30}. That increase could contribute to strong remote replay, as cells representing recent novel experience would be easier to activate and would tend to have stronger connections among themselves. In our study, E1 was always more novel than E2. This may explain why awake, remote replay of E1 was present in as many as 44% of the candidate events in E2 and was as prevalent as local replay of E2.

The replay events we observed were present in both waking and more sleep-like states, but were of higher fidelity in the awake state when the animal had recently been in motion. This came as a surprise to us given previous results that suggested either similar fidelity of waking and sleep SWR reactivation¹² or somewhat better reactivation in sleep as compared to waking³¹. This apparent disparity may reflect the use of non-sequential co-activity measures in previous studies.

Our findings complement recent reports of memory-related activity in the human³² and rat³³ hippocampus. These studies reported that, during waking behavior, the hippocampus can express internally generated patterns related to previous experience. Those patterns were present across times scales similar to those seen during experience, however, and were thus distinct from the rapid replay of extended spatial sequences reported here. We speculate that

the higher rate awake replay we found could support our ability to retrieve memory sequences in much less time than was required for the initial experience.

Finally, while the causal link between replay and consolidation remains to be established, our results may have important implications for the processes that allow for the long term storage of new spatial and event memories. We know that the neocortex and the hippocampus can both show oscillatory, synchronized patterns of activity during sleep and sleep-like states^{15, 34, 35}. Our findings suggest that this coordination involves higher rate neural activity but a less faithful recapitulation of experience than waking events. Awake replay, in contrast, is likely to occur during a desynchronized neocortical state more closely associated with sensory processing³⁵. Awake replay may therefore lead to repeated and accurate recapitulations of recent experiences in neocortical networks, and thus more faithful memories for those experiences. Further, awake replay can reactivate a memory for a past experience in the midst of an ongoing experience, potentially facilitating the formation of associations that link multiple distinct events across long spans of time.

Methods

A distinct set of analyses of the data used in this study and the associated methods have been presented in a previous manuscript²⁰.

Data collection and pre-processing

Three male Long-Evans rats (500–600g) were food deprived and pre-trained to alternate in a linear track. This pre-training was performed in a different room from the recording experiments. After the animals alternated reliably for liquid reward (sweetened condensed milk), they were implanted with a microdrive array containing 30 independently movable tetrodes targeting CA3 and CA1/2, ²⁷ according to UCSF and NIH guidelines. One the days following surgery tetrodes were advanced to the cell layers. All neural signals were recorded relative to a reference tetrode in the corpus callosum. Following data collection electrode locations were identified histologically (see Supplementary Fig. 13 for example histological sections and a diagram of the targeted regions of CA1 and CA3).

Animals were introduced to W-track environment 2 (E2) either 3 (N = 1) or 6 (N = 2) days before being introduced to W-track environment 1 (E1), with two fifteen minute run sessions a day. Here we examined data from when animals were first introduced to E1 onward where animals ran two sessions in E1 followed by one session in E2. Animals were rewarded for performing a continuous alternation task^{20, 21}. Rapid learning in this task requires an intact hippocampus²². Animals performed the inbound portion of the task (left or right to center) at nearly 100% correct on all days and performed at above chance levels on the outbound portion of the task (center to left or right) beginning with the second day of exposure to E1.

Run sessions were flanked by 20 minute rest periods in a high walled black box (floor: 25 by 34 cm; walls: 50 cm tall). The W-tracks were 76 by 76 cm with 7 cm wide track sections. Tetrode positions were adjusted after daily recording sessions for all tetrodes that had poor

unit recordings. On rare occasions some tetrodes were moved before recording sessions, but never within four hours of recording.

Data were collected using the NSpike data acquisition system (L. Frank, J. MacArthur). An infrared diode array with a large and a small cluster of diodes was attached to the preamps during recording. Following recording, the animal's position on the track was reconstructed using a semi-automated analysis of digital video of the experiment. Individual units (putative single neurons) were identified by clustering spikes using peak amplitude and spike width as variables (MatClust, M. Karlsson). Care was taken to only cluster well isolated neurons with spike waveform amplitudes that were clearly stable over the course of the entire session. We were frequently able to use a single set of cluster bounds defined in amplitude and width space to isolate units across an entire 2–3 hour recording session. In the minority of cases where there was a slight shift in amplitudes across time, units were clustered only when that shift was coherent across multiple clusters and where plots of amplitude versus time showed a smooth shift. Thus, no units where part of the cluster was in the noise or was cut off at the recording threshold were clustered.

Analysis of neural data

Analyses were performed using custom software written in Matlab (Mathworks, Natick, MA). To measure place field locations we calculated the 'linearized' activity of each cell. The animal's linear position was measured as the distance in cm along the track from the reward site on the center arm. We then produced an occupancy normalized firing rate map using spike counts and occupancies calculated in 2 cm bins and smoothed with a 4 cm standard deviation Gaussian curve. Only times outside of sharp-wave ripples (SWRs; see below) were included. Place field peak rate was defined as the maximum rate across all spatial bins. A peak rate of 3 Hz or greater was required for a cell to be considered a place cell. The results were the same with the 5 Hz threshold used in previous reports^{17, 18}. Putative interneurons were identified based on spike width and average firing rate^{36, 37}, and were excluded from all analyses. The two dimensional occupancy-normalized spatial rate maps shown in Fig. 1 and the Supplementary Figures were constructed with 2 cm square bins of spike count and occupancy, both smoothed with a 2D Gaussian (8 cm stdev). Once again, all SWRs were excluded.

Sharp waves ripple events (SWRs) were identified based on peaks in the local field potential (LFP) recorded from one channel from each tetrode in the CA3 and CA1 cell layers. The raw LFP data were band-pass filtered between 150–250 Hz and the SWR envelope was determined using a Hilbert transform. The envelope was smoothed with a Gaussian (4 ms stdev). We initially identified SWR events as sets of times when the smoothed envelope stayed above 3 standard deviations of the mean for at least 15 ms on at least one tetrode. We defined the entire SWR as including times immediately before and after that threshold crossing event during which the envelope exceeded the mean. Overlapping SWRs were combined across tetrodes, so many events extended beyond the SWR seen on a single tetrode.

We similarly extract theta and delta activity from the band-pass filtered LFP (theta: 6–12 Hz; delta 0.5–4 Hz). We used a Hilbert transform to determine the envelope of both theta

and delta, smoothed both envelopes with a Gaussian (1 sec stdev) and computed the theta / delta ratio by dividing the magnitude of the smoothed theta envelope by the magnitude of the smoothed delta envelope. For each day we selected the CA3 tetrodes where the variance of the theta/delta ratio was highest and normalized the values to a mean of one to permit combining data across days.

Candidate replay events were defined as SWRs during which at least 5 place cells from the replayed environment fired at least one spike each. We determined the sequential representation of position seen during a candidate replay using a simple Bayesian decoder^{24, 25}. Each event was divided into 15 ms bins, and for each bin with at least one spike in it we calculated the spatial probability distribution:

$$P(X|N_1^C) = \frac{P(N_1^C|X)P(X)}{P(N_1^C)}$$

Where X is the set of all locations in the environment (using 2 cm bins) and N_1^C is a vector of spike counts for all C cells that had place fields in the environment. Bins without spikes cannot be decoded using this simple algorithm, so these bins were omitted from the analysis.

$P(N_1^C|X)$ was calculated using the approximation that different cells are independent:

$$P(N_1^C|X) = \prod_{i=1}^C P(N_i|X)$$

$P(N_i|X)$ is the probability, at each location in the track, that cell i fired N_i spikes. We estimated that probability based on the occupancy normalized rate maps for that cell and the assumption that spike counts are Poisson distributed. $P(X)$ was a uniform distribution across all spatial bins and was thus an uninformative prior. $P(N_1^C)$ was not estimated; instead $P(X|N_1^C)$ was normalized across X to sum to 1. Note that decoding was done between food well locations, but as the animal could move slightly beyond these locations, the 2D place field plots extend further than the linear distances used for decoding.

To determine if a given decoded sequence was unlikely to occur by chance we drew 10,000 random samples from the $P(X|N_1^C)$ distribution for each decoded bin and assigned the sampled locations to that bin. We then performed a linear regression on the bin number vs. location points. The resulting R^2 value was then compared to 10,000 regressions where the order of the bins was shuffled. This shuffling preserved the spiking structure within each bin but ordered the bins randomly. This is equivalent to shuffling the order of the probability distributions over position produced from the decoding analysis (Supplementary Figure 14). The p-value for the event was the proportion of the shuffled R^2 values that was greater than the R^2 value of the actual event, and an event with $p < 0.05$ was considered to be unlikely to occur by chance. We obtained similar results when we shuffled the identity of each cell (e.g. assigned spike trains to randomly chosen neurons¹⁸; not shown).

We also developed a pair-wise measure of sequential activity consistent with replay. We measured, for every pair of cells, the absolute value of the time from each reference spike of one cell to all spikes from the other cell. Only spikes occurring during SWRs and only times up to 500 ms were included. We also measured the linear distance between the place field

peaks of the two neurons as the shortest path on the environment from the peak location for one cell to the peak location for the other cell. We then used a linear regression to calculate the R^2 value which measured the degree to which the distance between two cells' place fields predicted the absolute value of the time between SWR spikes from the cells. Each pair of cells was included only once.

We illustrated the quality of pair-wise reactivation using a method similar to that developed in a previous manuscript²⁸. We computed the cross-correlation histogram between SWR spikes from all pairs of neurons with place fields in the environment (5 ms bins, -500 ms to 500 ms extent). We constructed a two dimensional histogram plot where the time between spikes was on the X axis and the counts from each cross correlation histogram were a row placed at the distance between the centers of the two place fields. Thus, the correlogram for a pair of cells with identical place field peak locations would be a row of values at the bottom of the plot at a Y-value of zero, while the correlogram from two cells whose fields were 50 cm apart would be a row of values at a y-value of 50. Each row was normalized so that the peak and trough ranged from 0 to 1.

The similarity of spatial coding for single cells across the two environments was computed using place field overlap, defined as two times the sum of the overlapping areas of the linear rate curves divided by the sum of the areas of each curve³⁸. This measure is bounded between 0 and 1, where 0 signifies no overlap and 1 signifies perfect overlap. This is equivalent to rotating one of the tracks so that it lies entirely on top of the other and computing the similarity of linear place fields based on that rotation.

We determined whether replay of E1 and E2 was correlated by examining all replay events that were simultaneously E1 and E2 candidate events. Thus, each event had 5 or more E1 place fields and 5 or more E2 place fields active. As some cells were active in both environments, the total number of active cells was in some cases less than 10. We measured the R^2 value for the decoding of both E1 and E2 and used the shuffling described above to produce a p-value for both the E1 and the E2 cells. We computed the $-\log_{10}$ of the p values and calculated the correlation coefficient for the E1 and E2 transformed p values. We also examined candidate events for both E1 and E2 and asked whether the transformed p-value of the E1 replay was related to the number of E2 cells active.

We examined the effect of local spatial firing on remote replay for replay occurring both while the animal was in E2 and while it was in the rest box. For each significant replay event we identified the cell that fired the first spike and the cell that fired the last spike of the sequence. For E2 we used the linear place fields generated for the decoding to determine the rate of each cell at the animal's location. As indicated above, these place fields did not include SWR activity. For the rest box we similarly excluded SWRs and computed a 2D firing rate in 2 cm bins following smoothing with a 2D Gaussian (4 cm stdev). We then calculated the mean rates for the first and last cells across all significant events.

Supplementary Material

Refer to Web version on PubMed Central for supplementary material.

Acknowledgements

We thank Michael Brainard, Dan Feldman, Steve Lisberger, Michael Stryker and the members of the Frank laboratory for comments on the manuscript. We also thank Tom Davidson for a helpful discussion and Margaret Carr for help with histology photographs. This work was supported by the John Merck Scholars Program, the McKnight Scholars Program and NIH grants MH077970 and MH080283.

Reference List

1. Scoville WB, Milner B. Loss of recent memory after bilateral hippocampal lesions. *J. Neurol. Neurosurg. Psychiatry.* 1957; 20:11–21. [PubMed: 13406589]
2. O'Keefe, J.; Nadel, L. *The hippocampus as a cognitive map.* London: Oxford University Press; 1978.
3. Buzsaki G. The hippocampo-neocortical dialogue. *Cereb. Cortex.* 1996; 6:81–92. [PubMed: 8670641]
4. Sutherland GR, McNaughton B. Memory trace reactivation in hippocampal and neocortical neuronal ensembles. *Curr. Opin. Neurobiol.* 2000; 10:180–186. [PubMed: 10753801]
5. Suzuki WA. Encoding new episodes and making them stick. *Neuron.* 2006; 50:19–21. [PubMed: 16600852]
6. Wilson MA, McNaughton BL. Reactivation of hippocampal ensemble memories during sleep. *Science.* 1994; 265:676–679. [PubMed: 8036517]
7. Buzsaki G, Horvath Z, Urioste R, Hetke J, Wise K. High-frequency network oscillation in the hippocampus. *Science.* 1992; 256:1025–1027. [PubMed: 1589772]
8. Chrobak JJ, Buzsaki G. High-frequency oscillations in the output networks of the hippocampal-entorhinal axis of the freely behaving rat. *J. Neurosci.* 1996; 16:3056–3066. [PubMed: 8622135]
9. Buzsaki G. Hippocampal sharp waves: their origin and significance. *Brain Res.* 1986; 398:242–252. [PubMed: 3026567]
10. Csicsvari J, Hirase H, Mamiya A, Buzsaki G. Ensemble patterns of hippocampal CA3-CA1 neurons during sharp wave-associated population events. *Neuron.* 2000; 28:585–594. [PubMed: 11144366]
11. Pavlides C, Winson J. Influences of hippocampal place cell firing in the awake state on the activity of these cells during subsequent sleep episodes. *J. Neurosci.* 1989; 9:2907–2918. [PubMed: 2769370]
12. Kudrimoti HS, Barnes CA, McNaughton BL. Reactivation of hippocampal cell assemblies: effects of behavioral state, experience, and EEG dynamics. *J. Neurosci.* 1999; 19:4090–4101. [PubMed: 10234037]
13. O'Neill J, Senior TJ, Allen K, Huxter JR, Csicsvari J. Reactivation of experience-dependent cell assembly patterns in the hippocampus. *Nat. Neurosci.* 2008; 11:209–215. [PubMed: 18193040]
14. Lee AK, Wilson MA. Memory of sequential experience in the hippocampus during slow wave sleep. *Neuron.* 2002; 36:1183–1194. [PubMed: 12495631]
15. Ji D, Wilson MA. Coordinated memory replay in the visual cortex and hippocampus during sleep. *Nat Neurosci.* 2007; 10:100–107. [PubMed: 17173043]
16. Nadasdy Z, Hirase H, Czurko A, Csicsvari J, Buzsaki G. Replay and time compression of recurring spike sequences in the hippocampus. *J. Neurosci.* 1999; 19:9497–9507. [PubMed: 10531452]
17. Foster DJ, Wilson MA. Reverse replay of behavioural sequences in hippocampal place cells during the awake state. *Nature.* 2006; 440:680–683. [PubMed: 16474382]
18. Diba K, Buzsaki G. Forward and reverse hippocampal place-cell sequences during ripples. *Nat. Neurosci.* 2007; 10:1241–1242. [PubMed: 17828259]
19. Csicsvari J, O'Neill J, Allen K, Senior T. Place-selective firing contributes to the reverse-order reactivation of CA1 pyramidal cells during sharp waves in open-field exploration. *Eur. J. Neurosci.* 2007; 26:704–716. [PubMed: 17651429]
20. Karlsson MP, Frank LM. Network Dynamics Underlying the Formation of Sparse, Informative Representations in the Hippocampus. *J. Neurosci.* 2008; 28:14271–14281. [PubMed: 19109508]

21. Frank LM, Brown EN, Wilson MA. Trajectory encoding in the hippocampus and entorhinal cortex. *Neuron*. 2000; 27:169–178. [PubMed: 10939340]
22. Kim SM, Frank LM. Hippocampal lesions impair rapid learning of a continuous alternation task. *PLoS. ONE*. 2009 **In press**.
23. O'Keefe J, Recce ML. Phase relationship between hippocampal place units and the EEG theta rhythm. *Hippocampus*. 1993; 3:317–330. [PubMed: 8353611]
24. Brown EN, Frank LM, Tang D, Quirk MC, Wilson MA. A statistical paradigm for neural spike train decoding applied to position prediction from ensemble firing patterns of rat hippocampal place cells. *J. Neurosci*. 1998; 18:7411–7425. [PubMed: 9736661]
25. Zhang K, Ginzburg I, McNaughton BL, Sejnowski TJ. Interpreting neuronal population activity by reconstruction: unified framework with application to hippocampal place cells. *J. Neurophysiol*. 1998; 79:1017–1044. [PubMed: 9463459]
26. Johnson A, Redish AD. Neural ensembles in CA3 transiently encode paths forward of the animal at a decision point. *J. Neurosci*. 2007; 27:12176–12189. [PubMed: 17989284]
27. Frank LM, Stanley GB, Brown EN. Hippocampal plasticity across multiple days of exposure to novel environments. *J. Neurosci*. 2004; 24:7681–7689. [PubMed: 15342735]
28. Euston DR, Tatsuno M, McNaughton BL. Fast-forward playback of recent memory sequences in prefrontal cortex during sleep. *Science*. 2007; 318:1147–1150. [PubMed: 18006749]
29. de Hoz L, Wood ER. Dissociating the past from the present in the activity of place cells. *Hippocampus*. 2006; 16:704–715. [PubMed: 16888743]
30. Cheng S, Frank LM. New experiences enhance coordinated neural activity in the hippocampus. *Neuron*. 2008; 57:303–313. [PubMed: 18215626]
31. O'Neill J, Senior T, Csicsvari J. Place-selective firing of CA1 pyramidal cells during sharp wave/ripple network patterns in exploratory behavior. *Neuron*. 2006; 49:143–155. [PubMed: 16387646]
32. Gelbard-Sagiv H, Mukamel R, Harel M, Malach R, Fried I. Internally Generated Reactivation of Single Neurons in Human Hippocampus During Free Recall. *Science*. 2008
33. Pastalkova E, Itskov V, Amarasingham A, Buzsaki G. Internally generated cell assembly sequences in the rat hippocampus. *Science*. 2008; 321:1322–1327. [PubMed: 18772431]
34. Buzsaki G, Draguhn A. Neuronal oscillations in cortical networks. *Science*. 2004; 304:1926–1929. [PubMed: 15218136]
35. Mehta MR. Cortico-hippocampal interaction during up-down states and memory consolidation. *Nat. Neurosci*. 2007; 10:13–15. [PubMed: 17189946]
36. Frank LM, Brown EN, Wilson MA. A Comparison of the Firing Properties of Putative Excitatory and Inhibitory Neurons From CA1 and the Entorhinal Cortex. *J. Neurophys*. 2001; 86:2029–2040.
37. Fox SE, Ranck JBJ. Electrophysiological characteristics of hippocampal complex-spike cells and theta cells. *Exp. Brain Res*. 1981; 41:399–410. [PubMed: 7215500]
38. Battaglia FP, Sutherland GR, McNaughton BL. Local sensory cues and place cell directionality: additional evidence of prospective coding in the hippocampus. *J. Neurosci*. 2004; 24:4541–4550. [PubMed: 15140925]

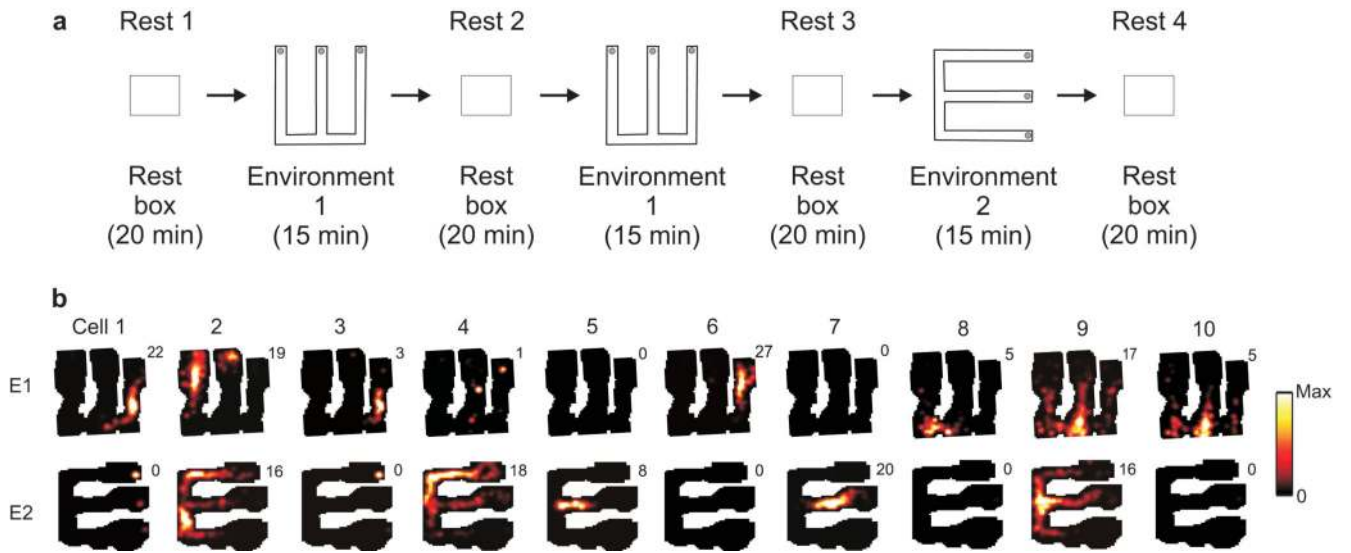


Figure 1.

a. Overview of experimental design. Each day of recording consisted of two 15 minute exposures to Environment 1 (E1) followed by one 15 minute exposure to Environment 2 (E2). Each exposure was flanked by 20 minute rest sessions in the rest box. The total size of each W-track was 76 cm square, and the width of the arms was 7 cm. The rest box was 25 × 34 cm. **b.** Distinct spatial representations for E1 and E2. Each column shows the spatial rate maps for one neuron for both E1 (top row) and E2 (bottom row). The number to the upper right of each plot corresponds to the maximum rate displayed for that cell which was 65% of the neuron's peak spatial rate. The color bars to the right illustrate the range of colors that are mapped from 0 to the maximum displayed rate. Rates are rounded to the nearest whole number. The plots show 10 of 33 simultaneously recorded neurons with E1 and/or E2 place fields from animal 3, day 8.

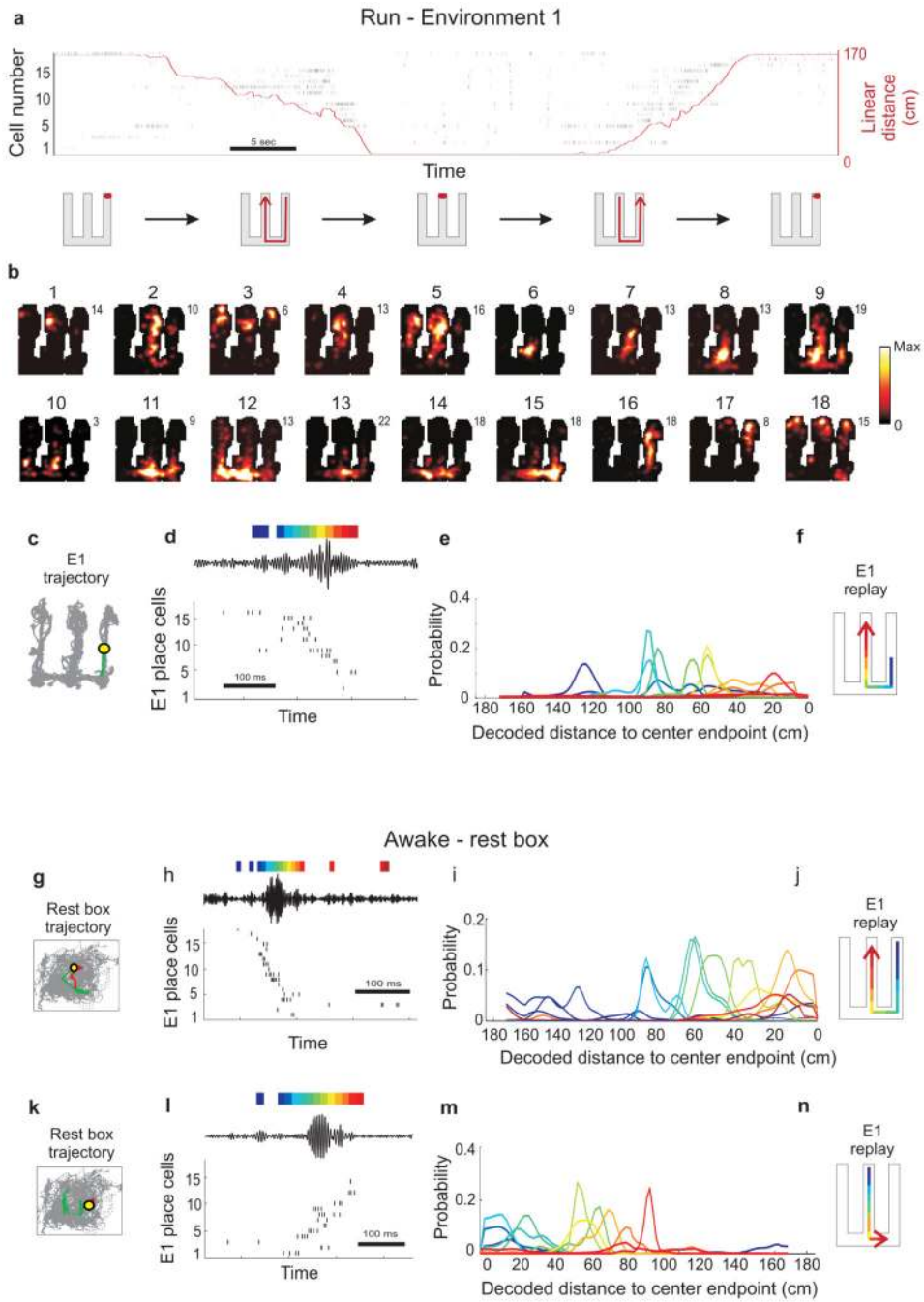


Figure 2. Spatially remote awake replay in the rest box. **a**, Spike rasters (black) from 18 cells active in E1 along a correct and a subsequent incorrect trajectory. The same cells and associated numbers are used in all panels. The red line shows the animal’s linear distance during the same period, and the W-track cartoons below show the specific locations the animal traversed. **b**, 2D spatial rate maps for the E1 place cells active in **(a)**. **c**, The animal’s trajectory during and after a replay event. Grey dots represent all sample locations, the yellow circle represents the animal’s location during the SWR and the green dots represent

the animal's location in the five seconds following the SWR. Here the animal was still for more than five seconds before the SWR, but in other figures red dots represent the locations during the five seconds before the SWR. **d**, Sequential spiking during the SWR. Bottom: rasters of all E1 place cells that were activated during the SWR. Top: the filtered LFP signal from one tetrode. The color bar shows the colors associated with each of the 15 ms decoding bins. **e**, Decoded locations for each bin. Each colored line represents the probability distribution resulting from decoding the spiking in the associated 15 ms period from (**d**). **f**, A cartoon of the replayed trajectory in E1. **g–j**, **k–n**. Examples of awake replay of E1 in the rest box. The motion before and after the events demonstrates that the animal was awake.

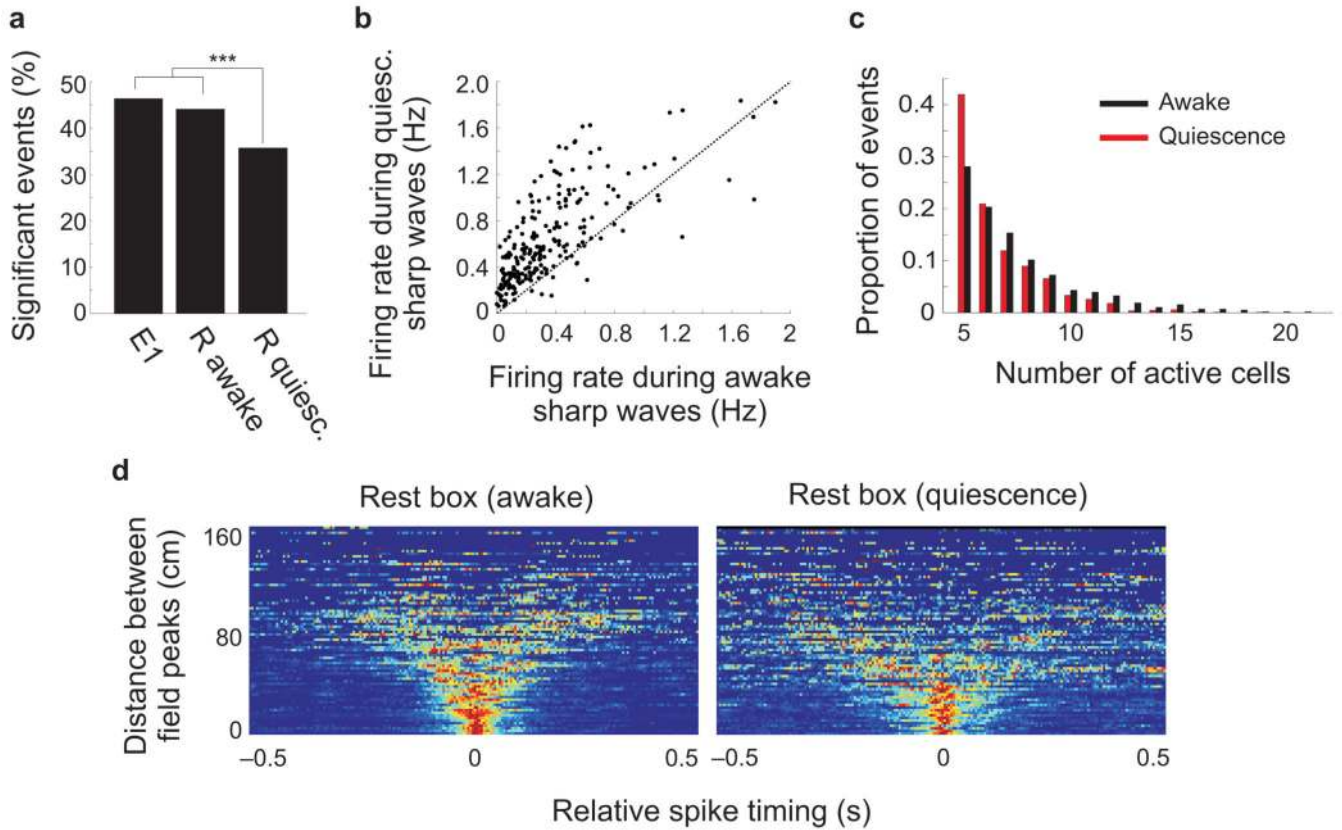


Figure 3.

Replay of E1 in the rest box is more robust during awake than quiescent periods. **a**, The proportion of significant replay events was similar in E1 and during awake periods in the rest box (R awake), but was lower during quiescence in the rest box (R quiesc.; $p < 0.001$). **b**, Scatter plot of the firing rate of all neurons with place fields in E1 during awake and quiescent SWRs in the rest box. Rates for the large majority of neurons were higher during quiescence ($p < 10^{-10}$). **c**, Histogram of the proportions of SWRs during awake and quiescent periods with different numbers of cells active. Awake SWRs were more likely to activate a larger number of cells as compared to while quiescent SWRs ($p < 10^{-10}$). **d**, Pairwise reactivation in the rest box. Each plot shows rows representing the normalized cross-correlograms between all pairs of simultaneously recorded neurons with place fields in E1, with the vertical location of each row determined by the distance between the two cells place field peaks in E1. The 'V' representing activation consistent with replay is more clearly visible in the awake state, and the R^2 value representing the degree to which the times between spikes from two neurons predict the distances between the peaks of their place fields was significantly larger for awake replay events.

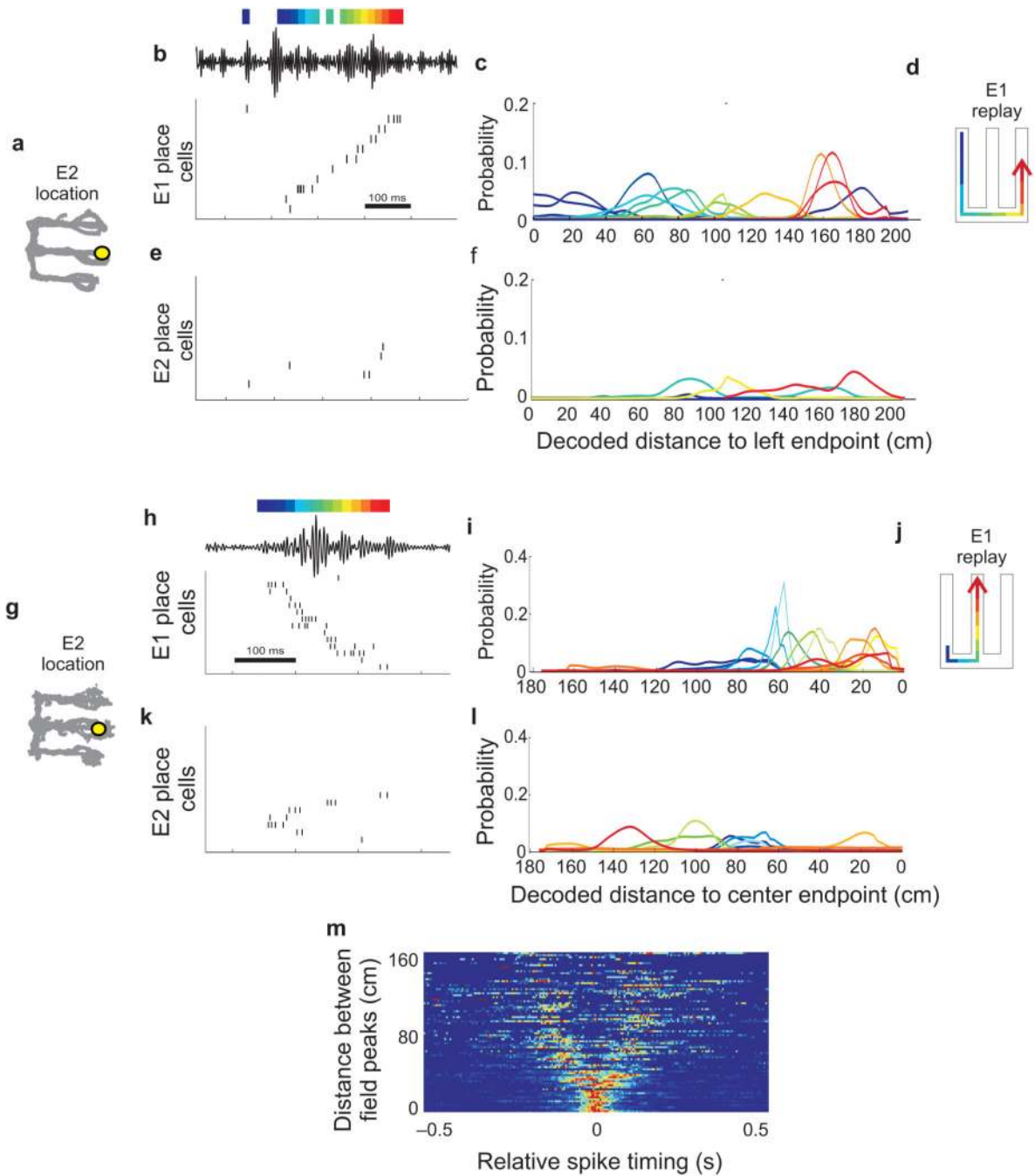


Figure 4.

Robust replay of E1 while the animal was located in E2. **a**, The location of the animal in E2 during an E1 replay event. **b**, Spiking during a SWR representing replay which decodes (**c**) to a coherent trajectory in E1 (**d**). See Fig. 2c–e for a detailed description of each element of the plots. For this event the animal was still for > 5 seconds before and after the SWR, so only the animal's location is shown in (**a**). **e**, **f**, Activation of neurons with place fields in E2 during the same SWR event and the decoded locations for E2. The neural activity during the SWR involved a coherent replay of E1 but not of E2. Cells are not numbered because

different subsets cells are shown in each panel, but cells with place fields in both E1 and E2 and are shown in both raster plots. See Supplementary Fig. 5 for this event and the associated 2D spatial rate maps. **g – i**. A second example illustrating replay of E1 in the absence of replay of E2. See Supplementary Fig. 6 for this event and the associated 2D spatial rate maps. See Supplementary Clusters for the cluster plots associated with each cell with a place field in E1. **m**, Pair-wise sequential activation plot for E2 SWRs including only neurons with place fields in E1 but not in E2. See Fig. 3d for an explanation of the plot. The associated R^2 value was 0.17, indicating activity consistent with replay.

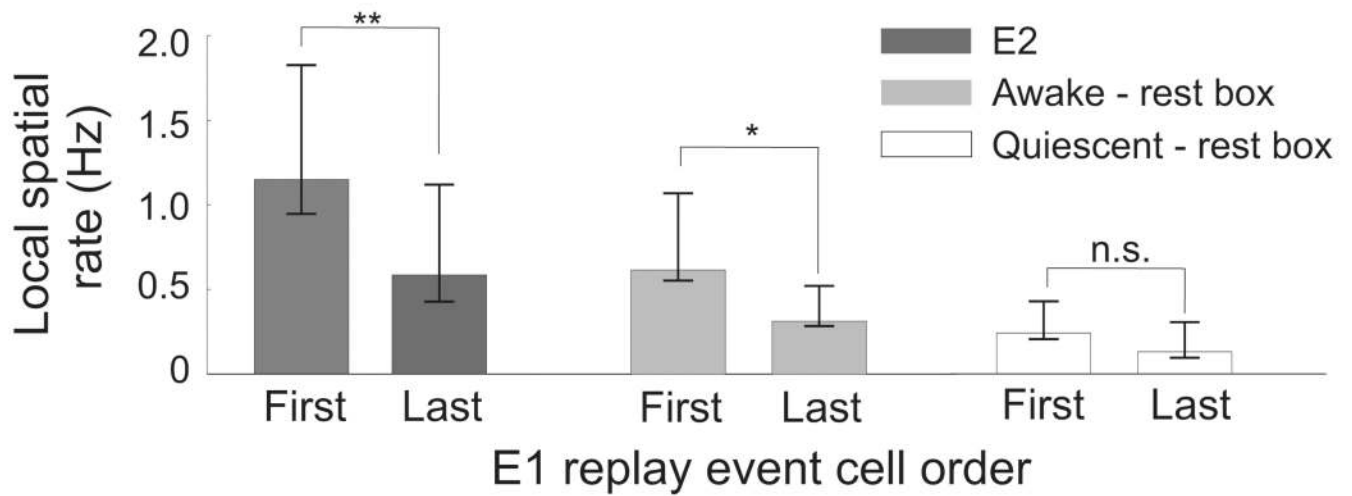


Figure 5.

Local spatial rate and replay initiation for E1 replay in E2 and the rest box. The first cell active in each SWRs had a higher local spatial rate in E2 and for awake (< 5 seconds immobile), but not quiescent (> 5 seconds immobile) events in the rest box. Error bars represents the mean \pm 25th percentiles. * represents $p < 0.05$, ** represents $p < 0.002$.